A Theoretical Model of Localized Heat and Water Vapor Transport in the Human Respiratory Tract

L. M. Hanna
Presently, School of Hygiene and Public Health, Johns Hopkins University, Baltimore, Md. 21205

P. W. Scherer

Department of Bioengineering, University of Pennsylvania, Philadelphia, Pa. 19104

A steady-state, one-dimensional theoretical model of human respiratory heat and water vapor transport is developed. Local mass transfer coefficients measured in a cast replica of the upper respiratory tract are incorporated into the model along with heat transfer coefficients determined from the Chilton-Colburn analogy and from data in the literature. The model agrees well with reported experimental measurements and predicts that the two most important parameters of the human air-conditioning process are: 1) the blood temperature distribution along the airway walls, and 2) the total cross-sectional area and perimeter of the nasal cavity. The model also shows that the larynx and pharynx can actually gain water over a respiratory cycle and are the regions of the respiratory tract most subject to drying. With slight modification, the model can be used to investigate respiratory heat and water vapor transport in high stress environments, pollutant gas uptake in the respiratory tract, and the connection between respiratory air-conditioning and the function of the mucociliary escalator.

Introduction

To prevent drying of the delicate interface of the alveolar capillary bed, inspired ambient air must be adjusted to body core temperature and full water saturation. This conditioning of the inspired air is accomplished as the airstream flows through the respiratory tract exchanging heat and water with the mucus membrane lining the airway surfaces. The process is remarkably stable over a range of inspiratory air temperatures between $-100°C$ and $500°C$ [23, 24]. The daily wide and sudden variations in ambient inspiratory conditions present a constantly varying thermal and fluid challenge which stresses the respiratory system, particularly the upper respiratory tract where most of the conditioning takes place.

The connection between respiratory air conditioning and respiratory disease lies largely in the dual role of the mucous membrane which acts as both the site of heat and water exchange and the protective interface between the environment and the respiratory tract. Pathenogenic organisms and particulates deposited in the respiratory tract are cleared from the system by ciliary motion which constantly propels the mucus out of the airways toward the epiglottis. The health and efficiency of this so-called mucociliary "escalator" is sensitive to changes in ambient air conditions. Serous and mucus secretion rates vary with temperature and humidity [18, 33] while the rheological properties of the secreted mucus are related to the net water loss or gain from the respiratory surfaces [19]. The motion of the mucous layer itself is dependent on the proper coupling between the hairlike projections at the distal ends of the cilia and the mucous layer. Excessive evaporation exposes more of the cilia to the viscous gel layer resulting in a large resistance to ciliary motion. An increase in the serous layer conversely can decouple the gel layer from ciliary contact. Within the pharynx there are relatively fewer mucus secreting cells or glands and the airway surface there is lined with unciliated squamous epithelial cells.

The inspired air-conditioning process does not occur uniformly throughout the respiratory system. Most of the respiratory air-conditioning occurs in the upper respiratory tract where as shown in a previous study [13], transport coefficients vary significantly as a function of longitudinal distance in from the mouth or nose. Knowledge of the local rates of heat loss and evaporation of water from the mucosal surface under varying ambient air conditions is essential to an ultimate understanding of health risks and local dysfunction of the mucociliary escalator.

A new steady state mathematical model of local human respiratory heat and water exchange is proposed in this paper from which local rates of heat and water vapor transport can be determined during inspiration and expiration as functions of distance into the airways. Utilizing experimentally measured local respiratory transport coefficients [13], the model reveals the most important parameters of the process, regional heat and water needs necessary to maintain the health of the respiratory mucosa, and new insight into the link between air conditioning efficiency and the vulnerability of the respiratory tract to disease.

Contributed by the Bioengineering Division for publication in the JOURNAL OF BIOMECHANICAL ENGINEERING. Manuscript received by the Bioengineering Division, June 16, 1984; revised manuscript received September 3, 1985.

Theoretical Model

Respiratory air-conditioning is a process occurring throughout the inspiratory and expiratory phases of the breathing cycle. The most efficient conditioning region is the nasal cavity, where during the normal breathing of room air, the temperature and humidity of the inspired air are raised to about 70 percent of body core temperature (37°C) and full water saturation at this temperature while the temperature of the nasal mucosal surface itself remains at only 32–33°C [7, 11, 25]. Airway wall temperature increases with distance away from the nose and at about the third bronchial generation the temperature of the airway mucosal surface approaches body temperature [9, 10, 28] as does that of the inspired air [9, 10]. The heat loss associated with the latent heat of vaporization of water evaporating from the surface is the most costly, contributing 85 percent of the total heat loss [34] and may result in a local drop in temperature of the heat mucosal surface.

During expiration, the driving forces for water and heat transfer are reversed and air at body core temperature and full water saturation flows between the bronchial tree and the nose or mouth losing heat and water to the cooler respiratory surfaces. The loss of heat from the airphase greatly decreases its water-carrying capacity due to the approximately exponential relationship between air temperature and full water vapor saturation [22]. The subsequent condensation of water at the mucosal surface results in a recovery of water and its associated latent heat amounting to 20–25 percent of the heat lost in inspiration. For quiet breathing of room air, the net loss per day in man as a result of the conditioning process is about 350 kcal of heat (15 percent of the basal metabolic heat generation) and 250–400 mL of water [5, 34].

That a quasi-steady state exists to a good approximation within the respiratory tract during the inspiratory and expiratory phases of the breathing cycle is strongly suggested by physiological data. Airstream temperature tracings at three different locations in the respiratory tract show that a steady state is established within at most 20 percent of the inspiratory time and even faster during expiration (Fig. 1) [6]. The tracings are not corrected for the time response of the thermocouples and would rise even faster if these corrections were included. Expiratory relative humidity tracings measured at the mouth also show a steady state to develop within 20 percent of the expired volume [12]. Similarly, studies of submucosal temperature show almost no fluctuation throughout the respiratory cycle [7, 17]. Furthermore, a characteristic length into the airways at and beyond which air temperature and humidity do not fluctuate over the respiratory cycle has been observed and called the Isothermal Saturation Boundary (ISB) [9]. The location of the ISB, at the second or third bronchial generation for normal respiration, is observed to shift with changes in ventilation rate, ambient air temperature and humidity, and tidal volume, consistent with a steady-state assumption.

Support for the steady-state assumption is also found by estimating the time required to set up steady thermal or mass

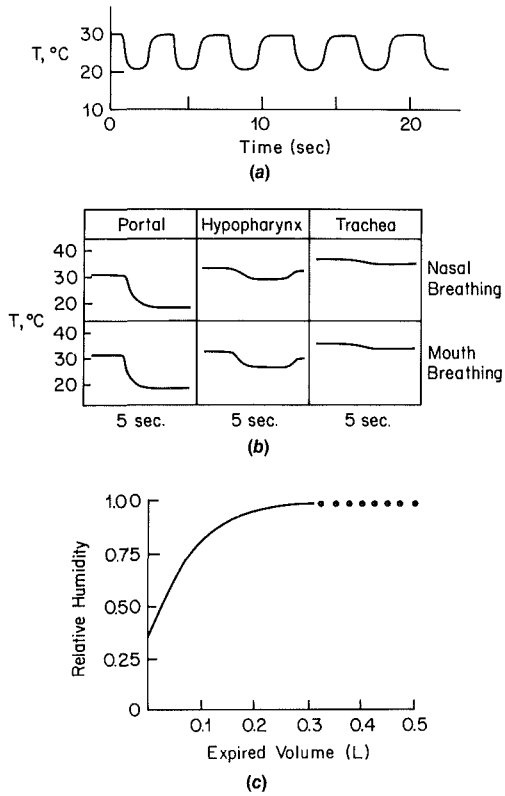

Fig. 1 *(a)* **Air temperature recording at the anterior nares of a subject breathing room air. Time interval is 5 s (6).** *(b)* **Recordings at different positions in the air passages (6).** *(c)* **Relative humidity of expired gas as a function of expired volume measured at the mouth during quiet breathing in a moderate environment. Delay and time constant corrections are included (12).**

concentration gradients within the airway walls. These characteristic times are of the order l^2/α where l is the linear distance from the capillary or venous bed in the wall to the air-mucus interface, and α is the thermal or mass diffusivity in the airway wall. Using estimates of l ($\simeq$ 50 μ) obtained from anatomic measurements, these times are seen to be very short ($\sim 10^{-3}$ s) compared to the time of inspiration ($\simeq$ 2.0 s), suggesting that wall temperature would not lag but would quickly adjust to sudden changes in air, blood or mucosal surface temperature. Furthermore, if all of the latter parameters were steady in time at a given position, so would be wall temperature. As noted in the foregoing, steady wall and air temperatures have been observed over most (the last 80–90 percent) of inspiration and expiration. A steady-state airway heat and water vapor transport model might therefore be expected to give reasonable agreement with experimental measurements.

The geometrical and physiological complexity of the respiratory system prevents a complete 3-dimensional analysis of airway heat and mass transport starting only from first

Nomenclature

A = airway cross section (cm^2)
C = water vapor concentration (moles/cm^3)
C_p = heat capacity at constant pressure (cal/g − °K)
D = diameter (cm)
h_c = heat transfer coefficient (cal/cm^2 − s − °K)
h_{fg} = latent heat of vaporizaiton (cal/g)
k = thermal conductivity (cal/cm − s − °K)
k_c = mass transfer coefficient (cm/s)
M = molecular weight
N = convective molar flux (moles/cm^2 − s)
Nu = Nusselt number
P = airway perimeter (cm)
Pr = Prandtl number
Re = Reynolds number
Sc = Schmidt number
Sh = Sherwood number
T = temperature (°K)
v = local air velocity (cm/s)
α = thermal or mass diffusivity (cm^2)
ρ = density of air (g/cm^3)

Subscripts

A = air
B = blood
M = mucus-air interface
N = naphthalene
t = tissue
W = water

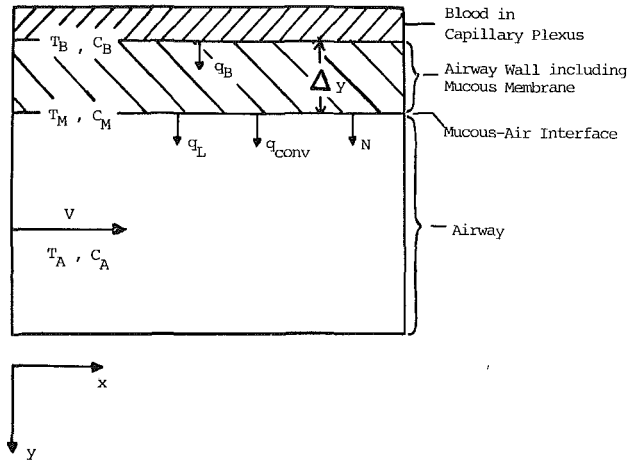

Fig. 2 Schematic diagram of the airway and control volume used to determine the heat and mass balances within any given region of the respiratory system and to derive equations (1)-(5). All quantities are functions of distance x along the airway.

principles. A local one-dimensional model of the conditioning process is possible, however, based on locally measured heat and mass transport coefficients. Recently, mass transport coefficients have been measured by the author in a model of the upper respiratory tract [13]. Measurements made in lower respiratory tract models have also been reported [17, 27].

A new quasi-steady theoretical model which describes for the first time local transport rates of heat and water vapor along the airways is shown schematically for inspiration in Fig. 2. To give the model full predictive capabilities, the choice of variables and parameters describing the air conditioning process must allow for flexibility in modeling of the various physiological and pathological changes in the respiratory system. At least five interrelated variables must be specified including: 1) the axially varying mixed-mean temperature, and water vapor content in the flowing air stream, T_A, C_A; 2) the mass flux rate of water vapor, N, from the mucousal surface into the flowing air stream; and 3) the temperature and water vapor content at the mucus-air interface, T_M, C_M. These five variables, together with local respiratory heat and mass transfer coefficients and a locally specified blood flow rate or blood temperature in the airway wall, completely determine the convective and conductive fluxes of heat and water at all points along the respiratory tract.

The theoretical model is derived by applying conservation of mass, momentum, and energy to a "slice" across the airway shown schematically for inspiration in Fig. 2. The resulting equations are as follows [31]:

$$\left(\frac{k_t}{\Delta y}\right)\left(T_B(x)-T_M(x)\right) = h_c(x)(T_M(x)-T_A(x))+\mathrm{NM}h_{fg} \quad (1)$$

$$N(x)=k_c(x)(C_M(x)-C_A(x)) \quad (2)$$

$$C_M(x)=22.4\exp(-4.9\times10^{-3}/T_M) \quad (3)$$

$$v(x)\frac{dC_A}{dx}=\frac{p(x)}{A(x)}k_c(x)(C_M(x)-C_A(x))$$

$$v(x)\frac{dT_A}{dx}=\frac{p(x)}{A(x)}\frac{1}{\rho C_{pA}}[h_C(x)(T_M(x)-T_A(x)) + C_{pW}M_WN(T_M(x)-T_A(x))] \quad (5)$$

Equation (1) is a statement of the energy balance at the air-mucosal interface in the steady state, where the conductive heat transfer from the blood to the mucus air interface is equal to the heat loss to the airphase by convection and evaporation (latent heat flux). We also assume that the energy gain to the airstream from the gaseous water flux is exactly balanced by a heat gain from liquid water flowing in from the blood such that these terms cancel out. It is also assumed that there is no frank drainage of water in the x direction.

Equation (2) is the definition of the convective water vapor flux, N, into the airstream where k_c is the local respiratory convective mass transfer coefficient. Values for k_c have recently been determined experimentally by measurements in a cast replica taken from a cadaver [13, 14].

Equation (3) is the thermodynamic equilibrium temperature versus water vapor concentration relation at the mucus-air interface. Initially the water vapor concentration as a function of surface temperature is assumed to be the saturation water vapor concentration above pure liquid water. Equation (3) is an accurate approximation to the Clausius-Clapeyron equation over a 15°C range near body temperature. In later computations, the mucus-water vapor pressure-temperature relation was allowed to vary in order to investigate the effect on air conditioning of mucosal water vapor pressures less than that of pure water.

Equations (4) and (5) are mass and energy balances in the x direction on the air phase portion of the "slice." Axial vapor diffusion is neglected. Heat and water transfer during the air-conditioning process are coupled due to the latent heat of vaporization in the evaporation of water from the mucosa. Consequently, equation (5) is nonlinear due to the dependence of the mass flux rate, N, on T_M and T_A through C_M and C_A.

Equations (1)–(5) constitute a system of five coupled nonlinear ordinary differential and algebraic equations for the five unknown functions, $N(x)$, $T_M(x)$, $C_M(x)$, $T_A(x)$, $C_A(x)$.

As shown in Fig. 2, the model is formulated using a mean blood temperature in the airway wall $T_B(x)$. Since very little experimental data is available on local airway wall blood flow rates or volumes, this formulation is simple but requires that $T_B(x)$ be known in order to solve equations (1)–(5). As is further discussed in the forthcoming, the model predicts that $T_B(x)$ is an extremely important parameter in the operation of the airway air-conditioning system.

The solution of the system of equations (1)–(5) provides a model of the steady-state temperatures, humidities, and heat and water vapor fluxes along the human respiratory tract during both inspiration and expiration. The equations must be solved numerically using appropriate values from the literature for $T_B(x)$, $A(x)$, and $P(x)$ (local airway cross section and perimeter), and $v(x)$ (local mean longitudinal air velocity). It is also necessary to know the values for the local respiratory heat and water vapor transport coefficients.

Localized Respiratory Transport Coefficients

During breathing in normal ambient environments, the respiratory mass transfer coefficients are more important to the air-conditioning process than the heat transfer coefficients because of the evaporation of water from the respiratory tract surface and its large associated latent heat loss. These mass transport coefficients are particulary important in the upper airway where most conditioning occurs. As noted in the foregoing, the latent heat loss amounts to 85 percent of the total heat lost during normal room air breathing. In a companion study [14], local upper airway mass transport coefficients were measured experimentally using the naphthalene sublimation technique in an acrylic cast model of the human upper airway.

In the experiments, the upper respiratory tract (except the nasal cavity) was divided into nine regions for each of which transport coefficients were evaluated using the naphthalene sublimation technique.

A respiratory heat transport coefficient within the nasal cavity was evaluated from physiological data. The nine regions considered were: 1, 2) the nasal cavity divided into

two regions, the turbinate region, and the region proximal to the turbinates; 3, 4) the nasopharynx divided into two regions; 5) the oropharynx; 6) the hypopharynx; 7) the larynx; and, 8, 9) 5 cm of the trachea which was considered as two separate regions.

In the naphthalene sublimation technique, naphthalene is the subliming vapor and the mass transfer coefficients measured for each region are those of an air-naphthalene vapor system. Local mass transfer coefficients for an air-water vapor system present in the respiratory air-conditioning process were evaluated using the Chilton-Colburn j-factor correlation (j_D for mass transfer). For the same flow geometry, the Sherwood number scales as the one-third power of the Schmidt number [3] or

$$\mathrm{Sh}_1 = \mathrm{Sh}_2 \left(\frac{\mathrm{Sc}_1}{\mathrm{Sc}_2} \right)^{1/3}$$

The equivalent diameter of a given local airway region (equal to four times the perimeter to cross-sectional area ratio) was used as the characteristic length in the nondimensionalizations.

A j-factor correlation for heat transfer exists similar to that for mass transfer which may be used to correlate heat transfer data. For flow in tubes [4], Colburn determined the empirical relation to be the j-factor scaled as the one-third power of the Prandtl number. When the physical properties of a gas are constant, when there is no source of heat or mass in the flow and relatively low rates of mass transfer are considered, an analogy exists (Chilton-Colburn analogy) between the transfer of mass and the transfer of heat such that the corresponding j-factors are equal [36]. Under these conditions, which are satisfied during respiratory conditioning, the local heat transfer coefficients for the resiratory geometry may be evaluated using the experimentally measured respiratory mass transfer experiments.

Within the acrylic model, as well as in the respiratory tract, the Schmidt numbers and the Prandtl numbers are within the range allowable [36] for use of the Chilton-Colburn Analogy ($0.6 \leq \mathrm{Sc} \leq 2500$, $0.5 \leq \mathrm{Pr} \leq 50$). Consequently, the j-factors for heat and mass can be equated. Expressing the j-factors in terms of the Sherwood and Nusselt number and equating them gives

$$\mathrm{Nu}/(\mathrm{Re}\,\mathrm{Pr}^{1/3}) = \mathrm{Sh}/(\mathrm{Re}\,\mathrm{Sc}^{1/3}) \tag{6}$$

Solving for the Nusselt number, assuming equal Reynolds numbers, then gives

$$\mathrm{Nu} = \mathrm{Sh}(\mathrm{Pr}/\mathrm{Sc})^{1/3} \tag{7}$$

as the relation between the dimensionless heat transfer coefficient, Nu, and the dimensionless mass transfer coefficient, Sh. At any given Reynolds number, the heat transfer coefficient may be determined from the measured mass transfer coefficient by use of equation (7).

The Sherwood numbers measured using the naphthalene sublimation technique were all determined for inspiration and at a single steady flow rate of 12 L/min through the upper airway model. In order to extend the Reynolds number range to which the mass transfer data can be applied, a complete heat, mass, and momentum analogy was assumed. To complete Chilton-Colburn analogy [36] between steady heat, mass, and momentum transfer when form drag is negligible states that

$$j_D = j_H = f/2 \tag{8}$$

where f is the friction factor and, for a given flow geometry, is a function of the Reynolds number only such that

$$f = g(\mathrm{Re}) \tag{9}$$

The j-factors therefore are also functions of the Reynolds number and have the same Reynolds dependency such that

Table 1 Inspiratory and expiratory coefficients of the Nusselt and Sherwood correlation equations for the regions of the upper respiratory tract model defined in the naphthalene sublimation experiments

Region of upper airway	Le	C_{Hi}	C_{He}
Nasal vestubule (nostrils)	2.0	0.056	0.017
Nasal cavity	4.0	0.056	0.017
Proximal to turbinates			
Nasal cavity	4.0	0.129	0.039
Turbinates			
Proximal nasopharynx	1.4	0.064	0.0207
Distal nasopharynx	1.9	0.032	0.0098
Oropharynx	2.3	0.046	0.0153
Hypopharynx	2.1	0.076	0.0254
Larynx	1.1	0.046	0.0146
Proximal trachea	2.7	0.032	0.0103
Distal trachea	2.8	0.045	0.0148

$$\begin{aligned} j_D &= c\,g(\mathrm{Re}) \\ j_H &= c\,g(\mathrm{Re}) \end{aligned} \tag{10}$$

where c is a constant.

Using the definitions of the j-factors in terms of the dimensionless variables, gives

$$\begin{aligned} j_D &= c\,g(\mathrm{Re}) = \mathrm{Sh}/(\mathrm{Re}\,\mathrm{Sc}^{1/3}) \\ j_H &= c\,g(\mathrm{Re}) = \mathrm{Nu}/(\mathrm{Re}\,\mathrm{Pr}^{1/3}) \end{aligned} \tag{11}$$

The Sherwood and Nusselt numbers can therefore be expressed as

$$\begin{aligned} \mathrm{Sh} &= c\,G(\mathrm{Re})\,\mathrm{Sc}^{1/3} \\ \mathrm{Nu} &= c\,G(\mathrm{Re})\,\mathrm{Pr}^{1/3} \end{aligned} \tag{12}$$

The functional dependence of the Sherwood number on the Reynolds number may be evaluated from a respiratory heat transfer correlation found by Nuckols [27] in a determination of an overall a heat transfer coefficient for the entire upper airway. His results showed that the Nusselt number scales approximately as the 0.856 power of the Reynolds number such that $G(\mathrm{Re})$ in equation (12) is given by

$$G(\mathrm{Re}) = \mathrm{Re}^{0.856} \tag{13}$$

The exponent in equation (13) is consistent with values for pipe heat transfer in swirling flow generated by airstream directional changes which were found to scale to the 0.8 power [15, 26]. The well-known Dittus-Boelter equation for the cooling of a fluid in fully developed nonswirling turbulent flow also expresses the Nusselt-Reynolds correlation as Reynolds number to the 0.8 power.

Assuming this same Reynolds dependency within each test region, the Nusselt and Sherwood numbers as a function of the Reynolds, Prandtl and Schmidt numbers are expressed from equation (12) as

$$\begin{aligned} \mathrm{Sh} &= C_{\mathrm{Hi}}\mathrm{Re}^{0.856}\mathrm{Sc}^{1/3} \\ \mathrm{Nu} &= C_{\mathrm{Hi}}\mathrm{Re}^{0.856}\mathrm{Pr}^{1/3} \end{aligned} \tag{14}$$

where the constant C_{Hi} (Hanna-inspiration) is the same for heat and mass transfer and is determined from the original naphthalene mass transport experiments. Using the local Reynolds number within each test region during the test runs and the experimentally determined local Sherwood numbers, the constant, C_{Hi}, within each test section is given by equation (14) as

$$C_{\mathrm{Hi}} = \mathrm{Sh}_N/(\mathrm{Re}^{0.856}\mathrm{Sc}_N{}^{1/3}) \tag{15}$$

where Sc_N is the Schmidt number for naphthalene vapor ($\simeq 2.5$). The values of C_{Hi} determined for each region are given in Table 1.

A correlating equation for the Sherwood and Nusselt numbers during expiratory flow in the respiratory tract may also be evaluated based on the locally measured inspiratory

mass transport coefficients. Nuckols' expiratory Nusselt-Reynolds-Schmidt correlation equation for nasal breathing [27] gives

$$G(\mathrm{Re}) = \mathrm{Re}^{0.984} \tag{16}$$

Similar to equation (14), the Sherwood and Nusselt correlations for expiration are therefore determined such that

$$\begin{aligned} \mathrm{Sh} &= C_{\mathrm{He}}\mathrm{Re}^{0.984}\mathrm{Sc}^{1/3} \\ \mathrm{Nu} &= C_{\mathrm{He}}\mathrm{Re}^{0.984}\mathrm{Sc}^{1/3} \end{aligned} \tag{17}$$

where C_{He} is, as in the inspiratory case, a constant to be evaluated. Since, however, no local expiratory mass transport coefficients were measured in the naphthalene sublimation experiments, a further assumption was necessary to obtain local Sherwood and Nusselt numbers for expiration.

To obtain a reasonable value of C_{He} for each region, a local expiratory Sherwood or Nusselt number was extrapolated from the inspiratory mass transport data. From Nuckols' inspiratory and expiratory heat transfer correlation for nasal breathing [27] it is seen that there is a Reynolds number at which the Nusselt number for inspiration is equal to the Nusselt number for expiration and which we will call the common Reynolds number. The Reynolds number used in Nuckols' correlations was determined using the tracheal diameter as the characteristic length. It was therefore assumed that, at the common Reynolds number within the trachea, the local Nusselt numbers within each region of the upper airway were also the same during inspiration and expiration.

The local Reynolds number for each test region, evaluated using the local equivalent diameter as the characteristic length, was determined at the common Reynolds number in the trachea. The local inspiratory Nusselt number at the common Reynolds number flow was then determined from the inspiratory Nusselt equation (14) for each region. Thus the coefficient, C_{He}, of equation (17) was calculated from the local Nusselt and Reynolds numbers evaluated at the common flow such that

$$C_{He} = \mathrm{Nu}_N/(\mathrm{Re}^{0.984}\mathrm{Pr}^{1/3}) \tag{18}$$

The values of C_{He} for each region are also given in Table 1.

In the lower respiratory tract, defined here as the mid-trachea to the terminal bronchioles, heat transfer coefficients have been evaluated by Johnson and Linderoth [17] for inspiratory flow in dogs as $\mathrm{Nu}_i = 0.259\ \mathrm{Re}^{0.785}\ \mathrm{Pr}^{1/3}$ and by Nuckols [27] for expiratory flow in a pipe bifurcation model as $\mathrm{Nu}_e = 0.0512\ \mathrm{Re}^{0.751}\ \mathrm{Pr}^{1/3}$. These Nusselt correlations are defined by both authors over a three generation model of the Weibel lung which is a symmetric dichotomously branching series of tubes. The characteristic diameter used in the nondimensionalization is the diameter of the first generation of each three generation bronchial compartment. The analogous lower respiratory mass transfer coefficients are evaluated at using the Chilton-Colburn analogy as described in the foregoing.

The foregoing scaling process provides local heat and mass transfer coefficients which can be used in the theoretical model for both inspiratory and expiratory flow under all physiological breathing conditions.

Results and Discussion of Computer Model Predictions

A fourth-order predictor-corrector numerical method was developed to solve the nonlinear equations (1)–(5). In the computer program the respiratory tract is modeled as a series of sequential compartments. The compartments of the upper respiratory tract correspond to the test sections where k_c was measured in the upper airway mass transport study [14]. The lower airway is made up of a series of compartments, each representing three generations of bronchial bifurcations. The inspiratory and expiratory transport coefficients were evaluated for each compartment as described in the previous section.

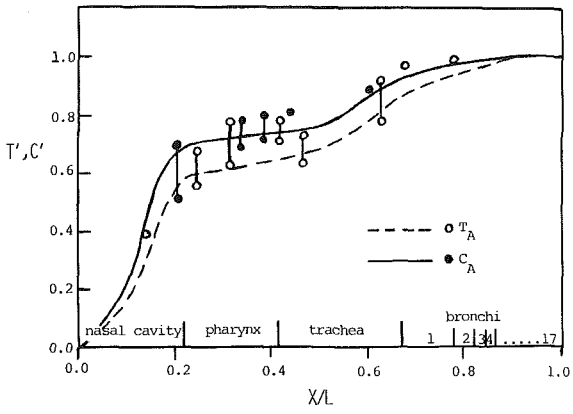

Fig. 3 Predicted nondimensional inspiratory temperatures and water vapor concentration profiles during room air breathing at rest plotted as a function of the nondimensional distance *x/L*. Room air breathing at rest is defined here as an inspiratory flow rate of 300 cc/s, an inspiratory temperature of 23°C and a relative humidity of 30 percent. The blood temperature $T_B(x)$ is set at 32°C in the nasal cavity, rising linearly distal to the nasal cavity at a rate of 0.33°C/cm, reaching body core temperature near the carina. Superimposed are the values of T_A' and C_A' determined experimentally within the human respiratory tract by various researchers [6, 8, 10, 16, 29, 30, 32, 35]. The characteristic length used to nondimensionalize the distance into the airways is measured from the nose to the 18th generation of Weibel's lung.

In the calculation, each compartment was treated as a separate segment with inlet conditions set equal to the outlet conditions of the preceding compartment. Within each compartment, the system of equations was solved at increments in Δx along the airways using the predictor-corrector method, the prescribed wall blood temperature and the known local anatomical measurements of $P(x)$ and $A(x)$. Values for the steady-state heat and water fluxes (q and N) were computed at each Δx as well as value of the mixed-mean temperature and humidity of the airphase and mucus-air interface.

The mixed mean airstream temperature as a function of distance into the airway was determined in dimensional $T_A(x)$ and nondimensional $T_A'(x)$ form. The nondimensional airstream temperature, $T_A'(x)$, is defined as

$$T_A'(x) = (T_A(x) - T_A(\mathrm{insp}))/(T_A(BT) - T_A(\mathrm{insp})) \tag{21}$$

where $T_A(\mathrm{insp})$ is the inspiratory ambient air temperature and $T_A(BT)$ is the body core temperature. T_A' indicates the fraction of conditioning achieved as a function of distance into the airways. The nondimensional water vapor concentration, $C_A'(x)$, is defined similarly.

The nondimensional blood temperature, $T_B'(x)$, is evaluated by replacing $T_A(x)$ in equation (21) with $T_B(x)$. The nondimensional blood temperature represents the value the nondimensional air temperature would have if the air temperature were always in equilibrium with the local wall blood temperature. The efficiency of the airway system to raise the inspired air to the wall blood temperature is visually apparent by observing the distance between the two curves $T_A'(x)$ and $T_B'(x)$. The nondimensionalized variables C_B', T_M', and C_M' are similarly defined. The axial distance into the airways, x, is nondimensionalized by the total length of the airway model.

Most of the existing physiological data on respiratory air conditioning has been measured during restful nasal breathing of room air. Mucosal and submucosal temperatures, and perimeter to cross-sectional area ratios as a function of distance into the airways are best known for these conditions. Single and multiple point determinations of airstream temperature and humidity within the human respiratory tract have been made by various investigators since the turn of the century [16, 30]. Reported airstream temperatures and humidities nondimensionalized using equation (21) (ambient air conditions of 23°C and 30 percent relative humidity are

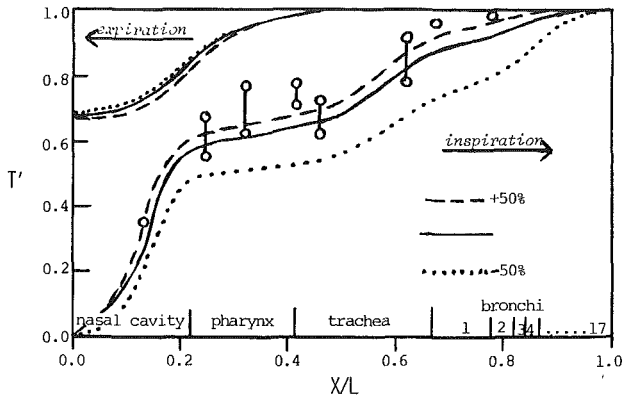

Fig. 4 Predicted nondimensional inspiratory and expiratory temperature profiles during room air breathing at rest plotted as a function of the nondimensional distance into the airway model. The transport coefficients are varied ± 50 percent throughout the airway model.

assumed since not all investigators reported the temperature and humidity of their room air) are shown in Fig. 3 plotted against the nondimensional distance into the airway. Differences in the "room air" inspiratory conditions used by the various investigators most likely contribute to the range of the in-vivo airstream data.

The computer model predictions during inspiration using physiological parameters for restful room air breathing [2, 12, 33] are also shown in Fig. 3. The model predictions fall well within the range of the experimental data [6, 8, 10, 16, 29, 30, 32, 35] with the exception of the two data points below the carina where Dery's [10] experimentally measured temperatures are greater than the model predictions. The difference is not very great (approximately 0.8°C and 0.2°C, respectively) and is most likely attributable to the difference in the inspired air temperatures between that used in the computer model predictions and those used during Dery's experiments which were simply referred to as "room air condition."

The effect of the transport coefficients, h_c k_c, on the predicted airway temperature and humidity profiles was evaluated by varying the coefficients by ±50 percent (Fig. 4). The change had almost no effect on the expiratory airstream temperature profiles. During inspiration, the nondimensional temperature profile was increased by less than 10 percent for the increased transport coefficients but still remain within the range of the experimental data. Lowering the coefficients produced a greater effect on the inspiratory profiles and reduced the temperature profile by about 25 percent in the nasal cavity.

The computer model predicts well both the airstream temperature profiles observed in vivo, and the movement of the aforementioned ISB, suggesting that the transport coefficients used in this study are reasonably accurate.

Figures 5 (*a*) and (*b*) shows the model prediction of the full conditioning process occurring within the airways for both inspiration and expiration. The water vapor concentration profiles predicted during nasal room air breathing at rest are shown in Fig. 5(*a*) for both inspiration and expiration and are compared with the blood equilibrium water vapor concentration profile. Within the nasal cavity the airphase nearly reaches equilibrium with the blood during both phases of the flow cycle indicating the efficiency of the nasal cavity to condition the air. The expiratory conditioning process results in a recovery of water as a result of the condensation of water onto the cooler nasal mucosa. Air is predicted to be expired at very near nasal blood temperature and full water vapor saturation at that temperature in excellent agreement with experimental data [6, 8, 10, 16, 24, 30].

After passage through the nasal cavity, during inspiration, the airstream reaches only 60–70 percent of body core

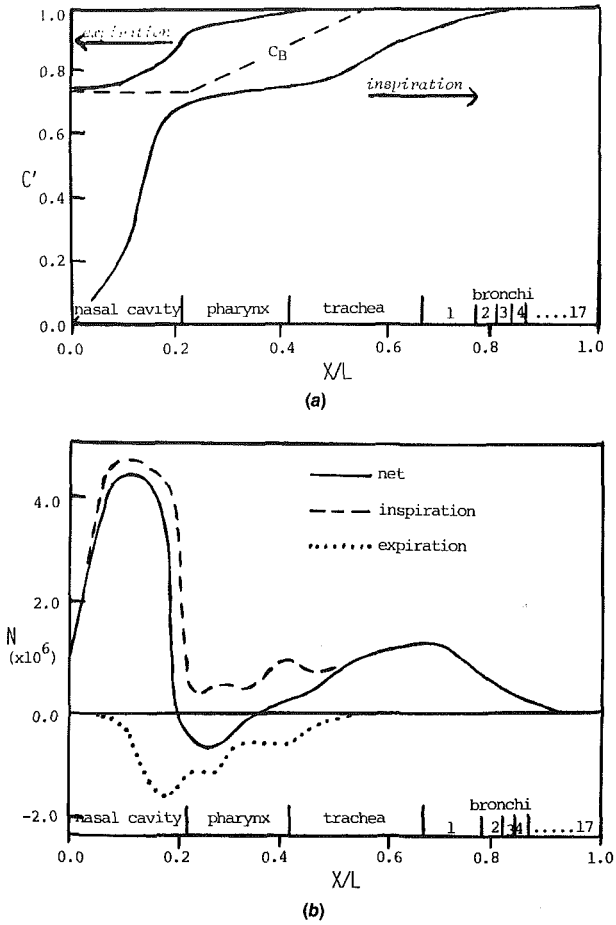

Fig. 5 Predicted inspiratory and expiratory profiles during room air breathing at rest as a function of distance into the airway model. (*a*) The nondimensional airway water vapor concentration profile and the water vapor concentration in equilibrium with the axial wall blood temperature, $C_B(x)$. (*b*) The inspiratory and expiratory water flux profiles, $N(x)$, in moles/cm^2-s, and the net water flux profile.

temperature and full water saturation. Relatively little conditioning of the inspired air occurs within the pharynx and upper trachea, thus requiring that the lower airways complete the conditioning process. As shown in Fig. 5(*a*), the upper tracheo-bronchial tree fully conditions the inspired air in a short distance and is seen to be the secondary major conditioning region of the respiratory system. A fact which is not widely appreciated.

The conditioning capabilities of the tracheo-bronchial tree are a result of the bifurcating tube structure which causes the total wall surface area to increase rapidly with distance into the airways. As the inspired air temperature decreases or the volumetric flow rate increases, less conditioning occurs within the nasal cavity due to a physiologically mediated drop in nasal blood temperature [7, 21]. Under these conditions, the model predicts that the tracheobronchial tree will play a relatively more important role in completing the conditioning process and protecting the lower respiratory tract from excess loss of heat and water. The significance of excess heat and water loss to the health of the lower tracheobronchial tree is becoming evident with recent deeper understanding of exercise-induced asthma [20] which is thought to be triggered by bronchoconstriction secondary to excess bronchial heat loss.

The local water demands on the respiratory tract mucosa can be seen from the water flux curves in Fig. 5(*b*) which correspond to the airstream water vapor concentration profiles shown in Fig. 5(*a*). Most of the conditioning of the inspiratory

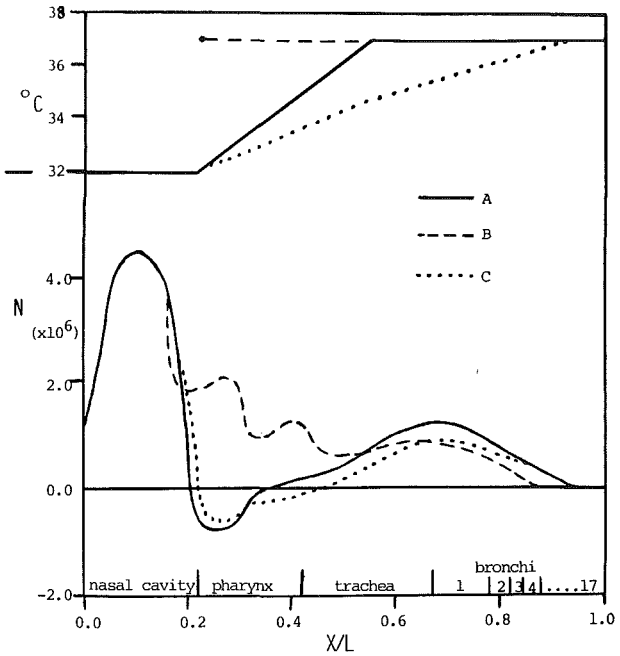

Fig. 6 Predicted net water flux profiles during room air breathing at rest while varying the wall blood temperature gradient distal to the nasal cavity. The wall blood temperature, $T_B(x)$, for the different cases is shown in dimensional form plotted as a function of distance into the airway model. Curve (A) is the same as the net flux curve in Fig. 5. A large effect on air conditioning in the pharynx produced by changes in $T_B(x)$ is shown.

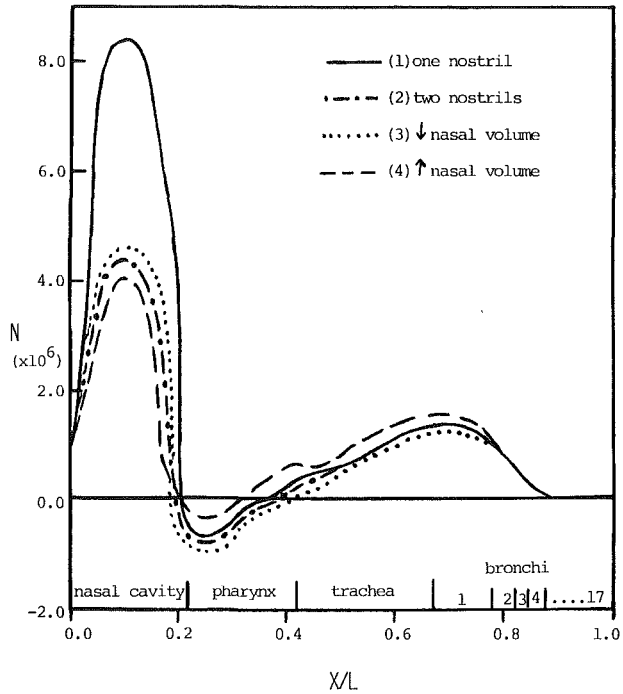

Fig. 7 Predicted net water flux profiles over one respiratory cycle during room air breathing at rest plotted as a function of the nondimensional airway distance. Results are shown for: (1) nasal breathing through one nostril at rest, (cross-sectional = 0.85 cm^2, perimeter = 8.0); 2) breathing through two nostrils; 3) decreased nasal volume, both nostrils (0.35 cm^2, 6.0cm); 4) increased nasal volume, (2.2 cm^2, 10.0cm). Cross sections and perimeters are those within one side of the nasal cavity.

airstream occurs within the nasal turbinates where large fluxes of heat and water occur due to the high degree of vascularization in the submucosa. The much smaller amount of inspiratory conditioning seen in the pharynx occurs for two reasons: 1) the air is very near the blood temperature during inspiratory flow through the pharynx due to the conditioning efficiency of the nasal cavity; and 2) the relatively low mass transfer coefficients within the pharynx are not conducive to high transport rates.

While inspiration results in water losses from the mucosa everywhere in the respiratory tract except in the distal regions of the lung, expiration can result in a gain of water proximal to the point where the wall blood temperature is below body core temperature (Fig. 5(*a*)). Consequently, the mucosa of the proximal trachea, larynx, pharnyx and nasal cavity can gain water on expiration. The amount of water gained in these regions depends on the difference between the local wall blood temperature and body core temperature.

Also shown in Fig. 5(*b*) is the net local water flux curve for all airway regions over one complete breathing cycle. For a given tidal volume and breathing frequency, the net flux is determined by assuming equal times for inspiration and expiration, and simply adding the inspiratory and expiratory fluxes at each point along the airways. Within the nasal turbinates, 50 percent of the water lost on inspiration is recovered during expiration. Of particular interest however is the net water flux within the pharynx which is seen to be negative, i.e., a net gain in water per cycle is predicted. This result has important health implications for the pharynx since the pharyngeal mucosa does not contain the mucus secreting cells and glands present in the rest of the system and may not be able to retain water efficiently. The geometrical design of the respiratory tract appears to be such that water is normally added to the pharyngeal mucosa over a breathing cycle to prevent drying.

The computer model was analyzed to determine the most sensitive parameters in the air-conditioning process. The nasal wall blood temperature and its gradient along the airways, and the perimeter to cross-sectional area ratio of the nasal turbinates, were found to be the most important parameters controlling both the airstream temperature and humidity profiles and the net heat and water fluxes as functions of distance into the respiratory tract.

Of all parameters varied within the possible physiological range, the wall blood temperature distribution, $T_B(x)$, was found to have the most significant effect on the net water flux throughout the respiratory tract (Fig. 6). When the blood temperature was set equal to body temperature immediately beyond the nasal cavity, the net water flux from the mucosa of the pharynx and larynx drastically increased (a maximum of 640 percent in the nasopharynx) due to the absence of water gain in these regions on expiration. The net flux in the bronchial tree was, however, somewhat reduced. Extending the blood temperature rise deeper into the bronchial tree (decreasing the wall gradient in $T_B(x)$) increases the mucosal region experiencing a net water gain and extends the conditioning process more distal into the bronchial tree. Similar results are obtained for the net heat flux as a function of distance into the respiratory tract.

Nasal volume changes are also seen, to influence the net heat and water losses in the pharynx by altering the cross-sectional area to perimeter ratio and thereby greatly affecting the conditioning efficiency of the nasal cavity. In Fig. 7, a decreased nasal cross-sectional area and perimeter, which results from a decreased nasal volume, results in a corresponding increase in the net heat flux within the nasal cavity with the inspired air being almost fully conditioned with respect to the nasal blood temperature.

Often, nasal resistance is decreased during exercise and hyperventilation, which is associated with an increase in nasal cross section. Under such conditions, the nasal cavity becomes a much less efficient air-conditioner as is also shown in Fig. 7. Considering the most extreme nasal volume for which the perimeter was assumed to increase, the air temperature

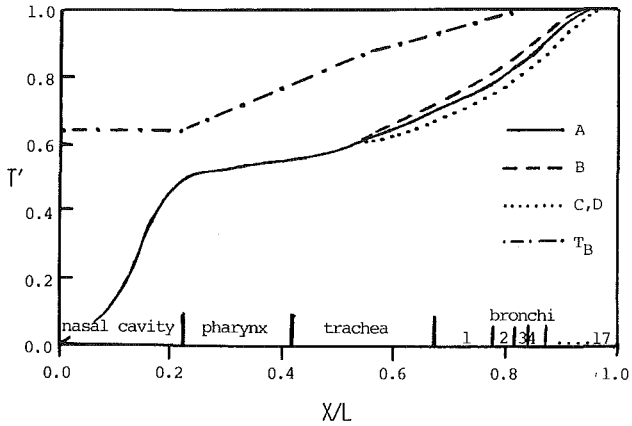

Fig. 8 Predicted inspiratory temperature profile at the maximum inspiratory flow rate of room air (2000cc/s) as a function of nondimensional airway distance (*a*) compared to: (*b*) 30 percent decrease in the lower airway compartments alone (bronchoconstriction); (*c*) an increase in the mucosal depth to 100μ, which also decreases the bronchial diameters, and the tissue thermal conductivity reduced to that of muscle (hypersecretion and muscularized bronchi often found in asthmatics); (*d*) both (*b*) and (*c*) in combination. The wall blood temperature, $T_B'(x)$ is also shown.

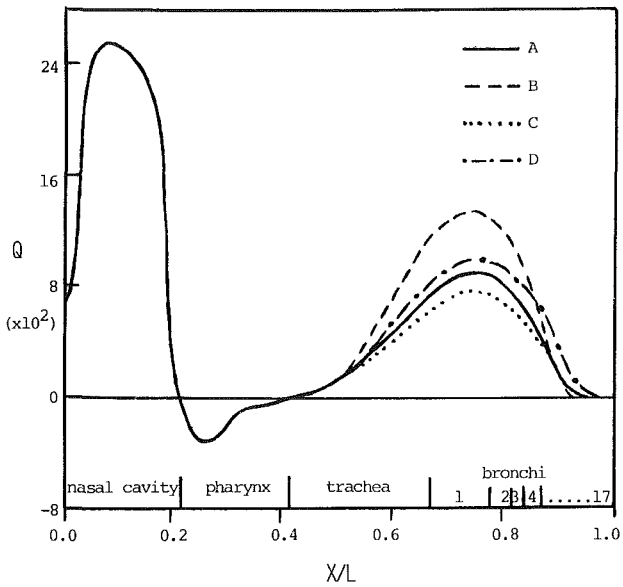

Fig. 9 Predicted net heat flux (cal/cm^2-s) profiles for maximal room air breathing (*a*) compared to: (*b*) bronchoconstriction (30 percent decrease); (*c*) hypersecretion (100 μ mucosal layer, tissue thermal conductivity reduced to that of muscle); and (*d*) both (*b*) and (*c*) in combination.

existing the posterior nasal cavity on inspiration is lowered 1.0°C. This results in an increased temperature and water vapor concentration gradient between the airstream and pharyngeal mucosa which increases the breath by breath inspiratory heat and water fluxes from the pharnyx.

Recently, much interest has been shown in the association between the bronchoconstriction of exercise-induced asthma and bronchial tree heat loss [20]. The computer model developed here offers an excellent approach to the study of this problem by allowing the major components of the asthma response, i.e., bronchoconstriction and hypersecretion, to be assesed independently. In Fig. 8, the predicted inspired air temperature profile, $T_A(x)$, during the maximum inspiratory flow rate is shown to vary only slightly depending on whether bronchoconstriction and hypersecretion were imposed individually or simultaneously. The effect is better evaluated however in Fig. 9 where the net heat flux profile gives the loss per unit surface area and shows a significant difference in heat flux for all cases.

Bronchoconstriction alone is seen in Fig. 9 to greatly increase the net heat flux within the bronchial tree (by 51 percent), increasing the inspiratory conditioning efficiency of the bronchi. An increased bronchial mucus layer (from 50 to 100 μ in thickness) and a reduced tissue thermal conductivity (0.09 to 1.19 $\times$ 10^{-3} cal/cm-s-°k assumed to result from the increased bronchial musculture thickness observed in asthma), reduces the net heat flux about 15 percent also reducing the conditioning efficiency within the region. Simultaneously, these two phenomenon combine to increase the heat loss by only 20 percent, thirty percent less than broncho-constriction alone. By slowing the heat and water losses, hypersecretion may therefore be a defense mechanism in response to the increased heat flux associated with bronchoconstriction.

Conclusions

The most sensitive parameters controlling the respiratory air conditioning process as predicted by the theoretical model are the airway wall blood temperature distribution, $T_B(x)$, and the nasal volume. Both of these parameters determine the local net heat and water flux throughout the respiratory system. This net flux is seen to be most changeable within the proximal pharynx where transition from a net gain to a net loss can easily occur. Often, changes in wall blood temperature and nasal volume are experimentally observed to occur simultaneously. These adjustments are a normal thermoregulatory response which changes the overall heat and water loss from the respiratory system. During the inspiration of cold air, a reduction in nasal blood temperature which does not vary in time over the respiratory cycle favors greater recovery of heat and water from the expired air.

The physical convective transport characteristics of the respiratory tract in combination with the physiological response of the blood temperature and nasal volume to various stimuli, appear to be purposefully designed to prevent or at least to minimize the net heat and water losses from the pharyngeal surface. This is accomplished by minimizing the role of the pharynx in inspiratory conditioning and maximizing the recovery of heat and water vapor during expiration which, in most cases, results in a net gain of water to the pharyngeal mucosa. The pharynx, which lacks both ciliated cells and glands, is particularly vulnerable to drying and irritation as evidenced by the high frequency of sore throats and upper respiratory infections arising in this region. It is interesting to speculate that changes in wall blood tempertaure are implicated in the development of these lesions. The inflammation associated with a sore throat most likely increases the local blood flow and therefore the local blood temperature resulting in increased pharyngeal mucosal inspiratory water losses, decreased expiratory water gains, and ultimately drying of the mucosal surface. Once dried, bacterial infiltration of the pharyngeal mucosa can proceed more easily.

The ability of the respiratory system to respond to the demands of inspiratory air-conditioning and still remain healthy appears to be most dependent on the axially varying wall blood temperature gradient and nasal volume changes. While some idea of nasal cross section may be obtained from nasal resistance measurements, very little information is available about axial wall blood temperature or its control.

The assumption was made at the beginning of these model studies that airway intra-wall blood temperature is near the mucosal surface temperature. This assumption is based on the fact that experimental determinations [7] of the submucosal temperatures yielded values similar to mucosal surface temperature measurements in other studies. In agreement with this assumption, the mathematical model presented here predicts that the mucosal temperature and the blood temperature are at least within 0.5°C of each other in the nasal

cavity and at least within 0.1°C of each other distal to the nasal cavity with the greatest differences occurring at the maximum flow rates.

This result has important implications for the study of the airway blood temperature response. Because of the small difference between surface mucosal and underlying wall blood temperature, the wall blood temperature may be accurately estimated simply by placing a thermoelement on the mucosal surface. Therefore by measuring mucus surface temperature, the blood temperature in response to various stimuli may be easily recorded.

Once the control of airway wall blood temperature and nasal volume is better understood, a theoretical model like the one described here can be used to investigate the connections between external stimuli and respiratory air-conditioning under normal and pathological conditions. This would be a valuable research tool which could ultimately be used to understand and prevent the development of respiratory tract infections and other respiratory disease processes.

References

1 Bird, R. B., Stewart, W. E., and Lightfoot, E. N., *Transport Phenomena*, Wiley, 1960.

2 Bowman, H. F., Cravalho, E. G., and Woods, M., "Theory, Measurement and Application of Thermal Properties of Biomaterials," *Annual Review of Biophysical and Bioengineering*, Vol. 4, 1975, pp. 43–80.

3 Chilton, T. H., and Colburn, A. P., "Mass Transfer (Absorption) Coefficients," *Industrial Engineering Chemistry*, Vol. 26, 1934, pp. 1183–1187.

4 Colburn, A. P., "A Method of Correlating Forced Convective Heat Transfer Data and A Comparison with Fluid Friction," *American Institute of Chemistry Engineering*, Vol. 29, 1933, pp. 174–210.

5 Cole, P., "Further Observations on the Conditioning of Respiratory Air," *Journal of Laryng.*, Vol. 65, 1953, pp. 669–681.

6 Cole, P., "Recordings of Respiratory Air Temperature," *Journal of Laryng.*, Vol. 68, 1954, pp. 295–307.

7 Cole, P., "Respiratory Mucosal Vascular Responses, Air Conditioning and Thermoregulation," *Journal of Laryng.*, Vol. 68, 1954, pp. 612–622.

8 Cramer, I., "Heat and Moisture Exchange of Respiratory Mucous Membrane," *Ann. Otol. Rhin. and Laryng.*, Vol. 66, 1957, pp. 327–343.

9 Dery, R., "The Evolution of Heat and Moisture in the Respiratory Tract During Anesthesia with a Non-Rebreathing System," *Canadian Aneasthesiology Society Journal*, Vol. 20, 1973, pp. 296–309.

10 Dery, R., Pelletier, J., Jacques, H., Clavet, M., and Houde, J. J., "Humidity in Anaesthesiology III: Heat and Moisture Patterns in the Respiratory Tract during Anaesthesia with the Semi-Closed System," *Canadian Anaesthesiology Society Journal*, Vol. 14, 1967, pp. 287–298.

11 Drettner, B., "Vascular Response of the Human Nasal Mucosa on Exposure to Cold," *Acta Otolaryngol.* (Stockh), Suppl. 166. 1961.

12 Ferrus, L., Guenard, H., Vardon, G., and Varene, P., "Respiratory Water Loss," *Resporatory Physiology*, Vol. 39, 1980, pp. 367–381.

13 Hanna, L. M., *Modelling of Heat and Water Vapor Transport in the Human Respiratory Tract*, Ph.D. thesis, Department of Bioengineering, University of Pennsylvania, Philadelphia, Pa., 1983.

14 Hanna, L. M., and Scherer, P. W., "Measurement of Local Mass Transport Coefficients in a Cast Model of the Human Upper Respiratory Tract," ASME JOURNAL OF BIOMECHANICAL ENGINEERING, Vol. 108, Feb. 1986, pp. 12–18.

15 Hay, N., and West, P. D., "Heat Transfer in Free Swirling Flow in a Pipe," TRANS. ASME, Ser. C., Vol. 97, 1975, pp. 411–416.

16 Inglestedt, S., "Studies on the Conditioning of Air in the Respiratory Tract," *Acta Oto-Laryng.*, Suppl. 131, 1956.

17 Johnson, C. E., and Linderoth, Jr., L. S., *Deep Diving Respiratory Heat and Mass Transfer*, School of Engineering, Duke University, 1976.

18 Keal, E. E., "Physiological and Pharmocological Control of Airways Secretions," *Respiratory Defense Mechanisms*, Vol. 5, Pt. I, eds., J. D. Brain, D. F. Proctor, and L. M. Reid, Marcel Dekker, Inc., 1979.

19 Litt, M., "Mucus Rheology," *Archives of International Medicine*, Vol. 126, 1970, pp. 417–423.

20 McFadden, Jr., E. R., Denison, D. M., Waller, J. F., Assouf, B., Peacock, A., and Sopwith, T., "Direct Recordings of the Temperatures in the Tracheobronchial Tree in Normal Man," *Journal of Clinical Investigation*, Vol. 69, 1982, pp. 700–705.

21 Malcolmson, K. G., "The Vasomotor Activities of the Nasal Mucous Membranes," *J. Laryngol. Proceedings*, Vol. 73, 1959, pp. 73–98.

22 Moore, W. J., *Physical Chemistry*, 4th edition, Prentice-Hall, Inc., 1972.

23 Moritz, A. R., Hendriques, F. C., and McLean, R., "The Effects of Inhaled Heat on the Air Passages and Lungs – An Experimental Investigation," *M. J. Path.*, Vol. 2, 1945, pp. 311–331.

24 Moritz, A. R., and Weisinger, J. R., "Effects of Cold Air on the Air Passages and Lungs," *Archives of Internal Medicine*, Vol. 75, 1945, pp. 233–240.

25 Mudd, S., Grant, S. B., and Goldman, A., "The Etiology of Acute Inflammations of the Nose, Pharynx and Tonsils," *Journal of Lab. Clinical Medicine*, Vol. 6, 1921, pp. 253–275.

26 Narezhnyy, E. G., and Sudarez, A. V., "Local Heat Transfer in Air Flowing in Tubes with a Turbulence Promotor at the Inlet," *Heat Transfer-Sov. Research*, Vol. 3, 1971, pp. 62–66.

27 Nuckols, M. L., *Heat and Water Vapor Transfer in the Human Respiratory System at Hyperbaric Conditions*, Naval Coastal Systems Center Technical Report TR364-81, Sept. 1981.

28 Ohgimi, T., Akiyama, S., and Shimokata, K., "Measurement of Surface Temperature in Lung Cancer," *Chest*, Vol. 81, 1982, pp. 62–66.

29 Perwitzschky, R., "Temperature and Moisture of Air and Air Passages," *Arch. Ohr. Nas. a. Kehlkopf.*, Vol. 117, 1927, pp. 1–35.

30 Proctor, D. F., and Swift, D. L., "Temperature and Water Vapor Adjustment," *Respiratory Defense Mechanisms*, Vol. 5, Pt. I, eds., J. K. Brain, D. F. Proctor, and L. M. Reid, Marcel Dekker, 1979.

31 Scherer, P. W., and Hanna, L. M., "Heat and Water Transport in the Human Respiratory System," *Heat Transfer in Biological Systems: Analysis and Application*, eds., Eberhardt and Shitzer, Plenum Press, 1985.

32 Seeley, L. E., "Study of Changes in Temperature and Water Vapor Content of Respired Air in Nasal Cavity," *ASHVE*, Vol. 51, 1940. pp. 377–388.

33 Sturgess, J. M., "Mucous Secretions in the Respiratory Tract," *Pedia. Clinic of N.A.*, Vol. 26, 1979, pp. 481–501.

34 Walker, J. E. C., Wells, Jr., R. E., and Merrill, E. W., "Heat and Water Exchange in the Respiratory Tract," *American Journal of Medicine*, Vol. 30, 1961, pp. 259–267.

35 Webb, P., "Air Temperature in Respiratory Tracts of Resting Subjects in Cold," *Journal of Applied Physiology*, Vol. 4, 1951, pp. 378–382.

36 Welty, J. R., Wicks, G. E., and Wilson, R. E., *Fundamentals of Momentum, Heat, and Mass Transfer*, 2nd Edition, Wiley, 1976.